LRP 353/88 August 1988

MEASUREMENTS OF THE TOKAMAK SAFETY FACTOR PROFILE BY MEANS OF DRIVEN RESONANT ALFVEN WAVES

H. Weisen, G. Borg, B. Joye, A.J. Knight,
J.B. Lister

MEASUREMENTS OF THE TOKAMAK SAFETY FACTOR PROFILE BY MEANS OF DRIVEN RESONANT ALFVEN WAVES

H. Weisen, G. Borg, B. Joye, A.J. Knight, J.B. Lister

Centre de Recherches en Physique des Plasmas
Association Euratom - Confédération Suisse
Ecole Polytechnique Fédérale de Lausanne
21, av. des Bains, CH-1007 Lausanne/Switzerland

ABSTRACT

We report on the first measurements of the safety factor profile in a tokamak using the dispersion properties of Alfvén waves. The waves were launched using the TCA Alfvén-wave heating antennae, which allowed the resonant excitation of Alfvén waves with defined mode numbers. The associated density oscillation profiles provided the shear Alfvén-wave resonance layer positions which, for non-zero poloidal mode numbers, depend on the local value of the safety factor, q. Our results for sawtoothing discharges with different plasma currents show a time-averaged q-profile with a flat central region where q is within a few percent of unity.

The safety factor profile is one of the most important parameters in theories of tokamak confinement, stability and transport. It remains, however, difficult to measure accurately. Previous measurement techniques have involved the use of Zeeman splitting of the atomic levels of an injected lithium beam[1] and the Faraday rotation of a far-infrared laser beam.[2] In this letter we present a novel method of measuring the safety factor profile by means of driven resonant Alfvén waves. Unlike previous techniques, in which the safety factor profile is deduced from the poloidal field profile, the present method is directly sensitive to the helicity of the poloidal field lines.

The use of resonant Alfvén waves to measure the safety factor profile in a tokamak has been suggested previously.[3] These waves may be launched by an external antenna structure, which defines the toroidal mode number, n. The poloidal mode number of the excited wave, m, is not uniquely defined by the antenna because of toroidal coupling. An Alfvén resonance is excited wherever the local Alfvén velocity matches the externally imposed wave velocity, $\omega/k_{//}$. In the large aspect ratio cylindrical approximation, $k_{//} = (n + m/q(r))R^{-1}$, where $q(r)$ is the local safety factor and R is the major radius. The resulting resonance condition can be written as

$$\omega^2\rho(0) = K[n + m/q(r)]^2/[\rho(r)/\rho(0)] \ , \qquad (1)$$

where $\rho(r)$ is the local mass-density. The constant, K, is given by

$$K = (B_\phi^2/\mu_0 R^2)(1 - \omega^2/\omega_{ci}^2) \ , \qquad (2)$$

where B_ϕ is the static toroidal magnetic field and ω_{ci} is the ion-cyclotron frequency. Equation (1) defines a frequency that is a function of the radius, $\omega(r)$, forming a continuous spectrum from a minimum, ω_{min}, which can be on- or off-axis, to a maximum value at the plasma edge. If n, m and $\rho(r)$ are known then the measurement of the resonance frequency as a function of radius for $m \neq 0$ can give a measurement of the safety factor profile, $q(r)$.

If, on the other hand, the driving frequency is held fixed, Eq. (1) defines a minimum threshold density, $\rho_{min}(0)$, above which a given (n,m) mode can be resonant. Any density higher than this threshold will move the resonance to a different radial position. The resonance layer position can be measured by observing the strong density oscillation which is excited in the region of the resonance layer by kinetic effects. This oscillation was first described by Hasegawa and Chen,[4] who showed that mode conversion from the magnetosonic wave launched by the antenna produces a radial propagating wave, the kinetic Alfvén wave (KAW). The KAW typically has a radial wavelength of a few centimetres. The existence of this wave in a tokamak has been experimentally confirmed on TCA.[5]

In order to extract the q-profile from one resonance profile, we would need an accurate measurement of $\rho(r)$. However, when the

line-densities for which the resonance condition is satisfied at a given radius are known for two identical discharges, with, for example, $(n,m) = (1,1)$ and $(2,0)$ excitation, the local value of q can be obtained directly. To see this, we rewrite the resonance condition (Eq. (1)) as

$$\omega^2 \rho_0 \, \rho^*(r) \propto [n + m/q(r)]^2 \, , \tag{3}$$

where ρ_0 is the central mass-density and $\rho^*(r)$ is the mass-density profile normalised to its value at $r = 0$. We assume that $q(r)$ and $\rho^*(r)$ do not change differently for the $(1,1)$ and $(2,0)$ cases during the density rise. This allows us to write Eq. (3) with $(n,m) = (1,1)$ and $(2,0)$ and solve for the safety factor to obtain,

$$q(r) = [2(\rho_{01}/\rho_{02})^{1/2} - 1]^{-1} \, , \tag{4}$$

where ρ_{01} and ρ_{02} are the values of the central density obtained when the $(1,1)$ and the $(2,0)$ modes are resonant at a given radius, r. The ratio of ρ_{01} and ρ_{02} can be obtained from electron line-density measurements, assuming that the $(1,1)$ and the $(2,0)$ discharges have the same effective ion mass, $\rho(0)/n_e(0)$. To ensure this condition the ohmic discharge was disturbed as little as possible by using a minimal RF power to excite the waves.

The waves were launched using the Alfvén-wave heating antennae on the TCA tokamak, whose parameters are; R, a = 0.61, 0.18 m, B_ϕ =

0.78—1.51 T, $I_p \leq 170$ kA and $n_e \leq 1.5 \times 10^{20}$ m^{-3}. The antennae consist of four toroidal groups of both top and bottom antennae.[6] The required mode numbers, $(n,m) = (1,1)$ and $(2,0)$, were determined by the relative phasing of the antenna groups. The RF power delivered to the plasma was about 40 kW, at a frequency of 2.04 MHz. The density oscillations were detected using a phase contrast imaging interferometer, which has been described in detail elsewhere.[7] A schematic diagram of the optical layout is shown in Fig. 1. The oscillations were detected using the driving signal of the RF generators as a phase reference. The associated circuitry and cabling introduced a further constant phase shift, which was not corrected since only an arbitrary phase reference was required.

Figure 2 shows the radial profile of the amplitude and phase of the line-density oscillation obtained for the same generator frequency and line-averaged electron density in both the (1,1) and (2,0) continua. The working gas was deuterium. Although the two continua were observed to have the same threshold density, the (1,1) resonance layer appears at a larger radius than the (2,0) layer at this density, somewhat above the threshold, as a result of its dependence upon the safety factor.

The effect of the q-dependence can be seen in the modelled curves of Fig. 3. This figure shows the positions of the resonant surfaces calculated using Eq. (1). The density profile was assumed to be of the form $n_e(r) = n_e(0)(1 - r^2/a^2)^{\alpha}$, with $\alpha = 1.2$ and the current density profile was assumed to be $j(r) = j(0)(1 - r^2/a^2)^{\beta}$,

where $\beta = q(a)/q(0) - 1$. The radial position of the $(n,m) = (2,0)$ resonance layer is independent of the q-profile, seen from Eq. (1). The same equation shows that the (1,1) resonance layer will be coincident with the (2,0) layer on-axis if $q(0) = 1$. The (1,1) layer profile is shown for three cases.Firstly, we take $q(a) = 3.2$ and $q(0) = 1.0$, for which the layers are coincident on-axis. Secondly we assume that $q(a) = 8$ and $q(0) = 1.0$. This curve indicates the effect of a narrow current profile with the same axial current density. Thirdly, we take $q(a) = 3.2$ and $q(0) = 0.7$. In these latter two cases, the resonance layer profiles are non-monotonic, with an off-axis threshold. For a certain range of density above the threshold, two resonant layers are present.

The excitation of Alfvén waves in the TCA tokamak always produces a density rise during the RF pulse. This density rise itself moves the resonance layers across the plasma radius, obviating the requirement to sweep the frequency in order to obtain the radial profiles of the resonance layers. The effect of this density rise can be clearly seen in Fig. 4. In this figure we have plotted the radial profile of the density oscillation amplitude for the (1,1) and (2,0) resonances as a function of the line-averaged electron density. The electron density was measured using a two millimeter interferometer aligned along a central chord. It can be seen that the positions of the resonances moved asymptotically towards the plasma edge as the density increased.

The exact radial position at which the resonance condition was

satisfied was found by comparing the measurements with numerical calculations of the kinetic Alfvén wave,[8,9] and in particular, calculations made using the ISMENE numerical code.[10] According to this code the resonance condition is satisfied at the point where the KAW completes its first half-cycle of propagation towards the plasma interior. This situation is favourable from an intrumental point of view because it corresponds to the viewing chord being practically tangential to the outer part of the shell-like KAW structure. The result is that the line-integrated signals give an accurate measurement of the radial dependence of the density oscillations without the need of an Abel inversion. The phase of the wave at the resonance position kept a constant relationship to the phase reference and it could be easily tracked throughout the density rise.

Some exceptions to this constant phase relationship were noted, and were due to the presence of radial standing waves, but such standing waves are limited to a narrow range of density near the thresholds of the resonances. They did not, therefore, introduce any significant uncertainties in the corresponding estimate of ρ_0. In such cases we directly used the amplitude data to provide ρ_0.

It is important to give a valid estimate of the accuracy of the q-profile, defined by the accuracy with which ρ_0 is estimated. In the case of standing waves, the uncertainty in ρ_0 was somewhat generously defined by the interval in density over which the

standing waves were observed. In the case of propagating waves, the error bars we have adopted corresponded, again very conservatively, to a margin of $\pm \pi/2$ in the phase, although the actual phase measurement was accurate to within a tenth of a radian. The error bars on subsequent figures indicate these uncertainties.

Figure 5 shows the measured positions of the resonance layers for the (1,1) and (2,0) modes plotted as a function of line-density. This measurement was obtained for a plasma current of I_p = 125 kA and a toroidal field of B_ϕ = 1.51 T. The difference in the rate of outward movement between the (1,1) and (2,0) resonances as the density increased clearly illustrates the q-dependence of the radius of the (1,1) layer. Although this discharge showed sawtooth behaviour, the ensuing modulation was not resolved in the measurements; the frequency response of the instrumentation provided an averaging over the sawtooth period.

Figure 6(a) shows the q-profile deduced from the measurement of the resonance positions of Fig. 5. The error bars in this figure indicate worst-case combinations of the line-density errors arising from the allowed phase error of $\pm \pi/2$. As the density increase at low power was often insufficient, on its own, to force the (2,0) resonance layer out to $r/a \gtrsim 0.7$, we have added extra points at larger radii by using the Abel inverted density profile from an eight-chord far-infrared interferometer (when available) together with the (1,1) resonance layer profiles. These are the

filled circles in Fig. 6. Figure 6(a) shows data taken from a sawtoothing discharge and exhibits a q-profile that is flat from $r/a = 0$ to $r/a \approx 0.4$. This radius corresponds, within one centimetre, to the sawtooth inversion radius[11] obtained from soft x-ray measurements. The profile extrapolates well to the cylindrically equivalent safety factor at the plasma edge, calculated via the relationship $q_I = 5\times10^6 a^2 B_\phi / R I_p$, in this case $q_I = 3.2$. The q_I points are indicated by the crosses in Fig. 6.

Figures 6(b) and (c) show the q-profiles for discharges with the same toroidal field as Fig. 6(a) but with plasma currents of 70 kA and 50 kA, respectively. Both these profiles also extrapolate well to the corresponding values of q_I, namely $q_I = 5.7$ and 7.9, respectively. These profiles do not have the flat central region shown in Fig. 6(a) and indicate a more peaked plasma current. Figure 6(b) shows q-values in the central region slightly above unity, while 6(c) has central q-values substantially above unity. Neither of these two discharges showed any sawtooth behaviour (the onset of sawteeth in TCA corresponds to $q_I \approx 5$).

Figure 6(d) shows the q-profile for a discharge with a reduced toroidal field of $B_\phi = 1.16$ T and a larger plasma current of $I_p = 135$ kA. The reduced toroidal field, together with the higher plasma current, caused the value of q_I to decrease to 2.3. Again, the measured q-profile extrapolates well to this value. The reduced edge value of the safety factor was not associated with a reduced central value, compared to the case of Fig. 6(a). However,

the central flat region has extended so that $q(r)$ stays close to unity out to $r/a \approx 0.5$. This distance corresponds to the increased sawtooth inversion radius, observed on the soft x-ray signals.

These results show safety factor profiles which are flat inside the sawtooth inversion radius where q is close to unity. This form of q-profile is consistent with the quasi-interchange model of the sawtooth collapse proposed by Wesson.[12] Our results add to the present dilemma regarding different measurements of the central value of the safety factor, and the implications which follow for various theories of the sawtooth oscillation.[13] Faraday rotation measurements on the TEXTOR[14] and JET[15] tokamaks have yielded $q(0)$ values significantly less than unity, 0.6 and 0.7, respectively, while measurements taken in TEXT[16] using the Zeeman effect have indicated a value of $q(0) \approx 0.7$. However results obtained from the ASDEX[1,17] tokamak displayed q-profiles similar to the present results, with $q(r)$ close to unity in the central region. This has also been indicated by observations of the "snake" phenomenon in JET after injection of a pellet into the plasma core.[18] In view of the diversity of results regarding the central q-value, we must assess our ability to measure a profile with a central safety factor significantly less than unity.

Figure 3 shows that the resonance layer profile with $q(0) = 0.7$ is non-monotonic for the (1,1) case. As a result its threshold is off-axis and occurs at a value of the central density which is 28% higher than the monotonic cases. The experimental

uncertainties are well below this amount. The (1,1) threshold has never been observed to occur at a line-density significantly higher than the (2,0) threshold. Therefore the central safety factor has never been indicated to lie below unity. In addition, in the case of the non-monotonic (1,1) resonance profile, the KAW would be propagating outwards from the inner resonance point. It could be detected as such, or if interference with the inwardly propagating KAW launched from the outer resonance point takes place, off-axis standing waves could result. Such standing waves at the (1,1) threshold have only been observed over a range of density of a few percent, and indicate only a slight non-monotonicity in an otherwise essentially flat (1,1) profile. Thus a central q-value as low as 0.7 has never been indicated by observations of the (1,1) resonance in TCA.

We have succeded in demonstrating the feasibility of measuring the q-profile using Alfvén waves. Natural extensions to the work described will be: the use of other mode pairs, such as (3,0) and (2,1); the use of a frequency sweep rather that a density sweep; and the time resolution of the q-profile evolution during the sawtooth cycle. Finally, the question of toroidicity should be addressed to confirm the absolute accuracy of the estimated q-profile.

ACKNOWLEDGEMENTS We are grateful for the support of the TCA team in this work, which was partly supported by the Fonds National Suisse de la Recherche Scientifique.

REFERENCES

[1] K. McCormick et al., Phys. Rev. Lett. 58, 491 (1987)

[2] H. Soltwisch, E. Graffman, J. Schlüter and G.Waidman, Proc. Int. Conf. on Plasma Physics, Lausanne, 1, 499 (1984)

[3] S.M. Mahajan, D.W. Ross, G.L. Chen and R.D. Bengston, University of Texas at Austin report #223 (1981)

[4] A. Hasegawa and L. Chen, Phys. Fluids, 19, 1924 (1976)

[5] R. Behn et al., Plasma Phys. Contr. Fusion, 26, 173 (1984)

[6] G.A. Collins et al., Phys. Fluids, 29, 2260 (1986)

[7] H. Weisen, Rev. Sci. Instrum. (to be published)

[8] D.W. Ross, G.L. Chen and S.M. Mahajan, Phys. Fluids, 25, 652 (1982)

[9] I.J. Donnelly, B.E. Clancy and N.F. Cramer, J. Plasma Phys., 35, 75 (1986)

[10] L. Villard, O. Sauter, K. Appert and J. Vaclavik, Int. Conf. on Plasma Physics, Kiev, 3, 172 (1987)

[11] G. Bateman, MHD Instabilities, MIT Press, Cambridge, Mass., (1978) p. 218

[12] J.A. Wesson, Plasma Phys. Contr. Fusion, 28, 243 (1986)

[13] J.A. Wesson in Theory of Fusion Plasmas, Proceedings of the Workshop held at Varenna, Italy, 1987, edited by A. Bondeson, E. Sindoni and F. Troyon, (International School of Plasma Physics, "Piero Caldirola", Milan, 1987) p. 253

[14] H. Soltwisch, W. Stodick, J. Manickam and J. Schlüter, Proc.

IAEA Conf., Kyoto, 1, 263 (1986)

[15] O'Rourke et al., in Procedings 15th European Conf. on Controlled Fusion and Plasma Heating, Dubrovnik, 1, 155 (1988)

[16] W.P. West, D.M. Thomas, J.S. de Grassie and S.B. Zheng, Phys. Rev. Lett. 58, 2758 (1987)

[17] McCormick et al., in Procedings 15th European Conf. on Controlled Fusion and Plasma Heating, Dubrovnik, 1, 35 (1988)

[18] Weller et al., Phys. Rev. Lett. 59, 2303 (1987)

FIGURE CAPTIONS

1. Schematic diagram of the optical arrangement to measure the density oscillations on TCA; AL: aperture limits of a CO_2 laser beam of width 23 cm, L: plasma limiter, WF: radial wavefronts of the KAW, Σ: object plane at the plasma equatorial plane, Σ': image plane, with 30 element HgCdTe photoconductive detector array (16 elements used), VL: viewing line for one of the elements.
2. Radial profiles of the synchronous line-density oscillations obtained at the same values of line-density and excitation frequency for (1,1) and (2,0).
3. Calculated radial positions of the (1,1) and the (2,0) resonance layers as a function of the central density.
4. The density fluctuation amplitude plotted as a function of line-density at 16 radial locations for the (1,1) and (2,0) discharges.
5. Resonance layer positions for the (1,1) and (2,0) modes as a function of the central line-density.
6. Safety factor profiles for (a) B_ϕ = 1.51 T, I_p = 125 kA, (b) B_ϕ = 1.51 T, I_p = 70 kA, (c) B_ϕ = 1.51 T, I_p = 50 kA, (d) B_ϕ = 1.16 T, I_p = 135 kA.

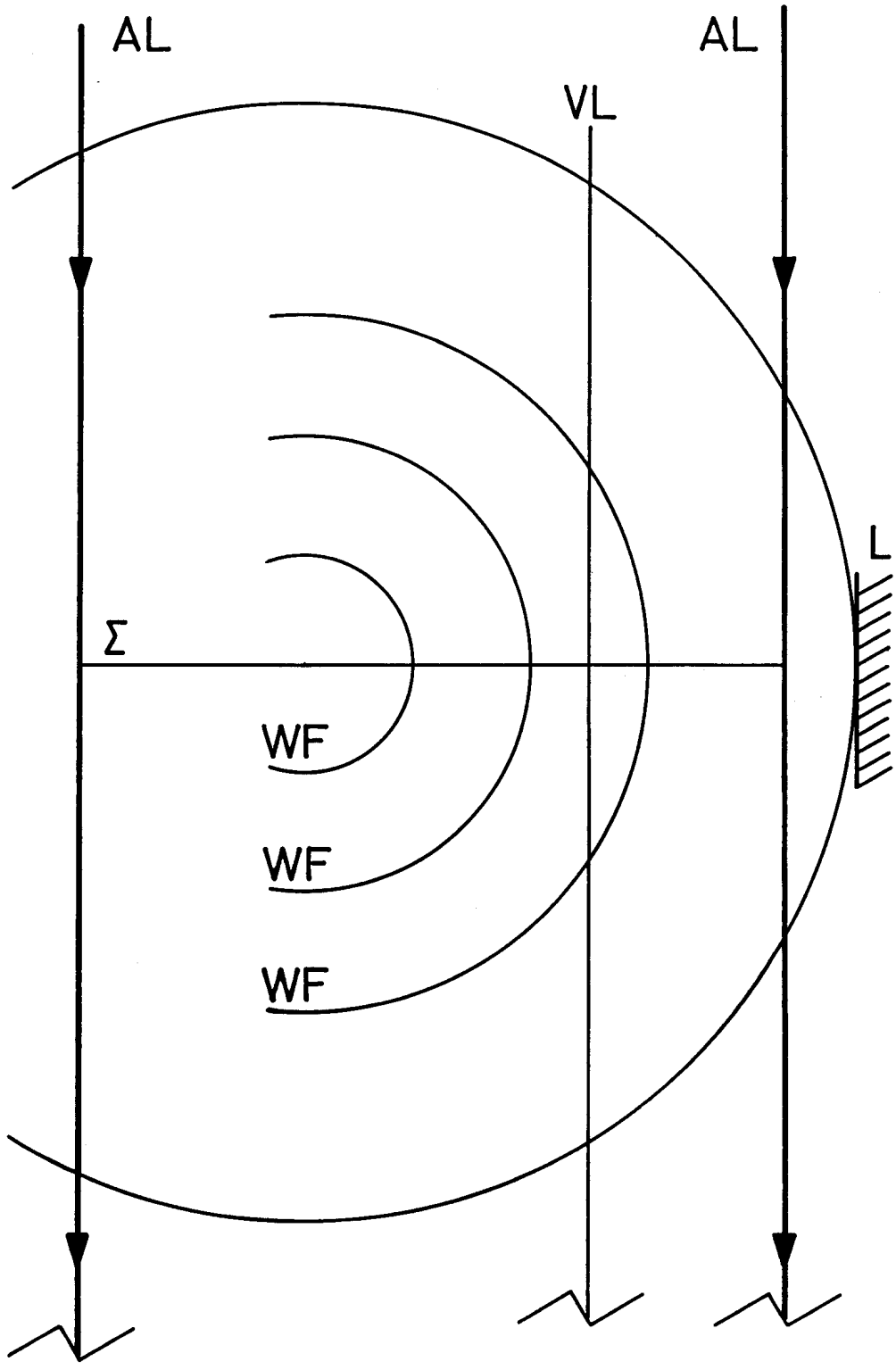

Imaging optics

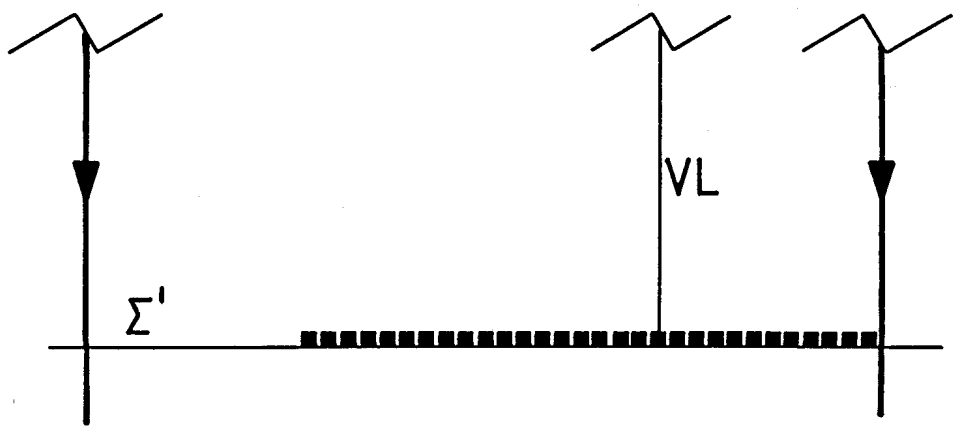

FIG 1

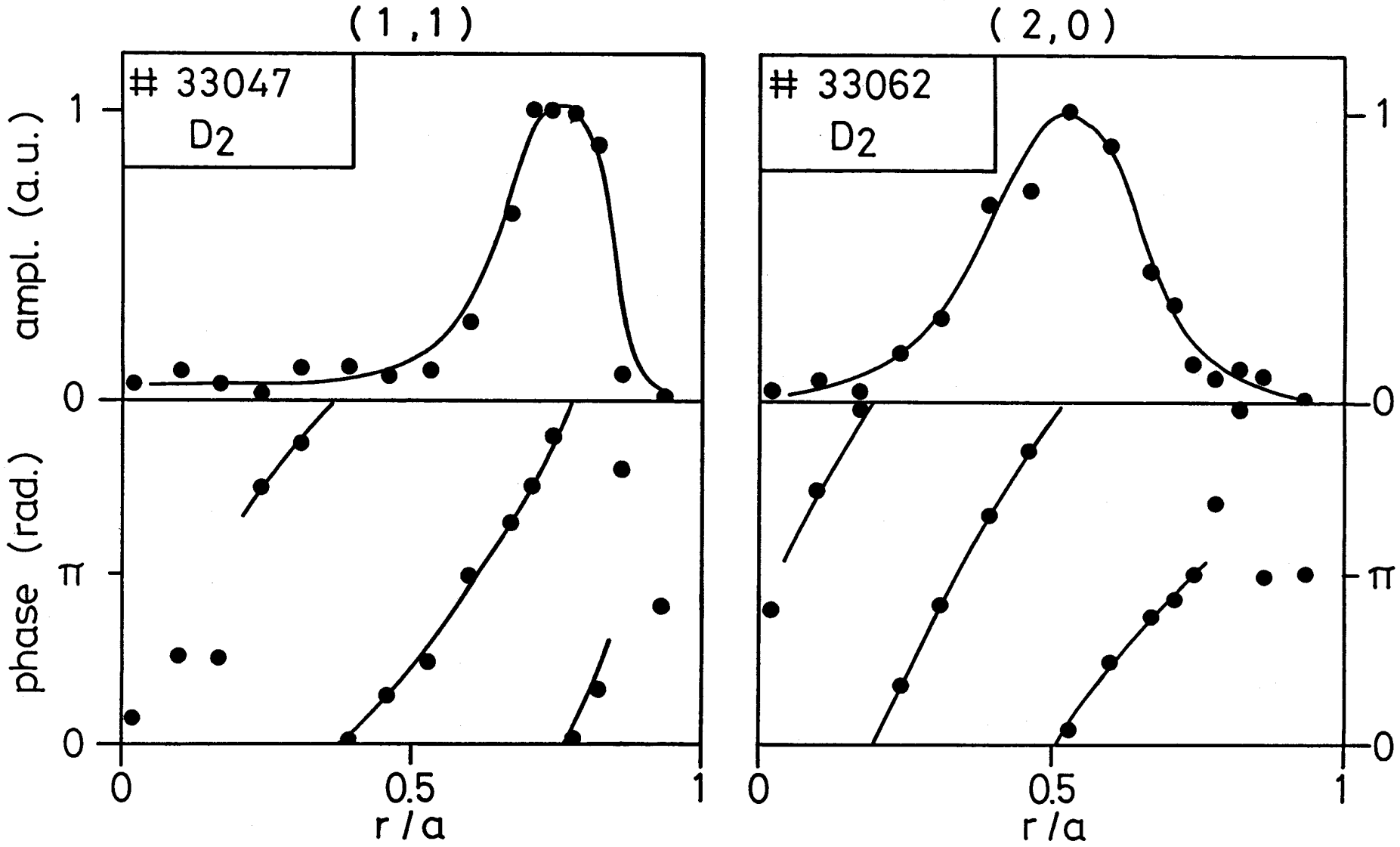

FIG 2

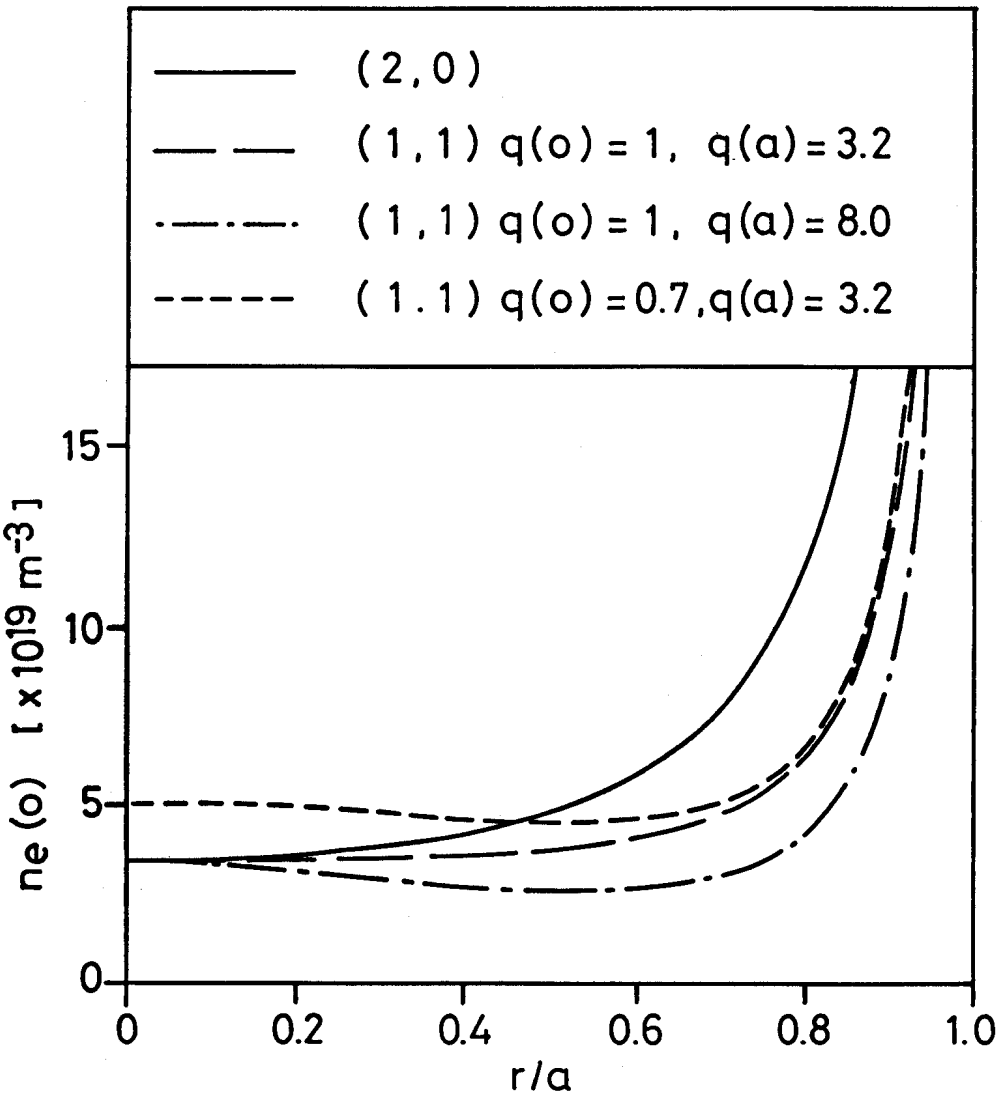
(2,0)
(1,1) q(o) = 1, q(a) = 3.2
(1,1) q(o) = 1, q(a) = 8.0
(1.1) q(o) = 0.7, q(a) = 3.2
ne (o) [x 10^19 m^-3]
15
10
5
0
0
0.2
0.4
0.6
0.8
1.0
r/a

FIG 3

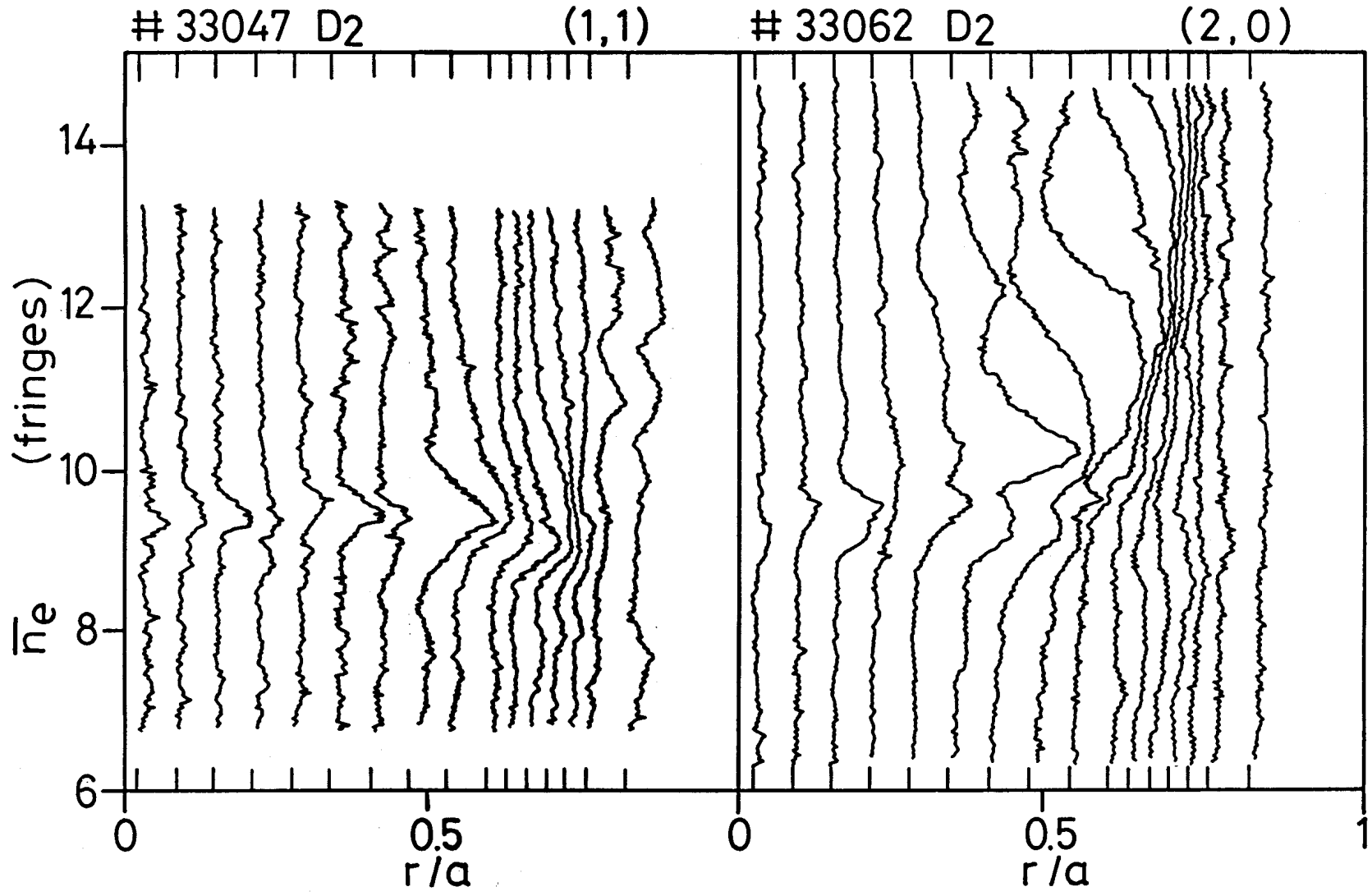

FIG 4

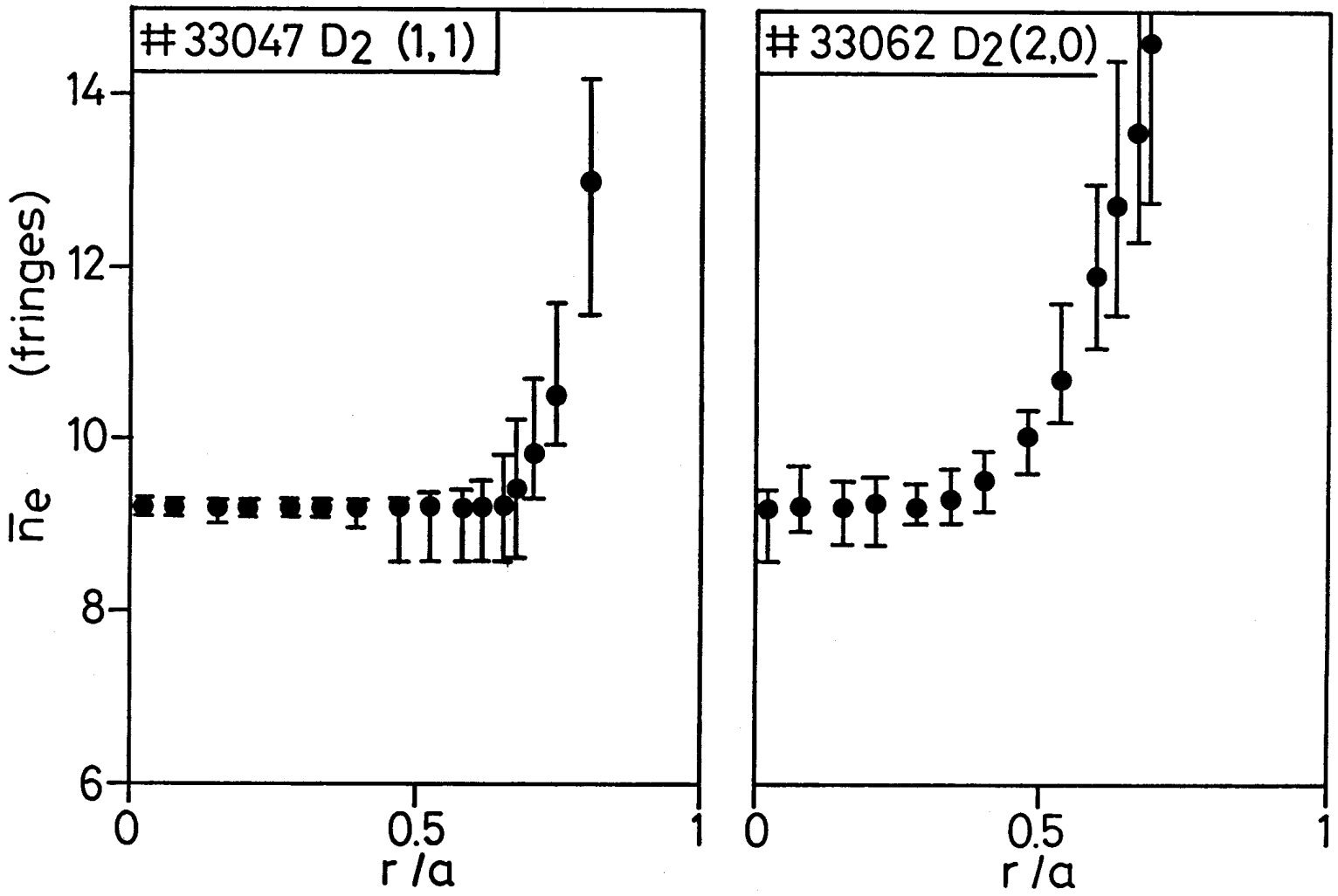

FIG 5

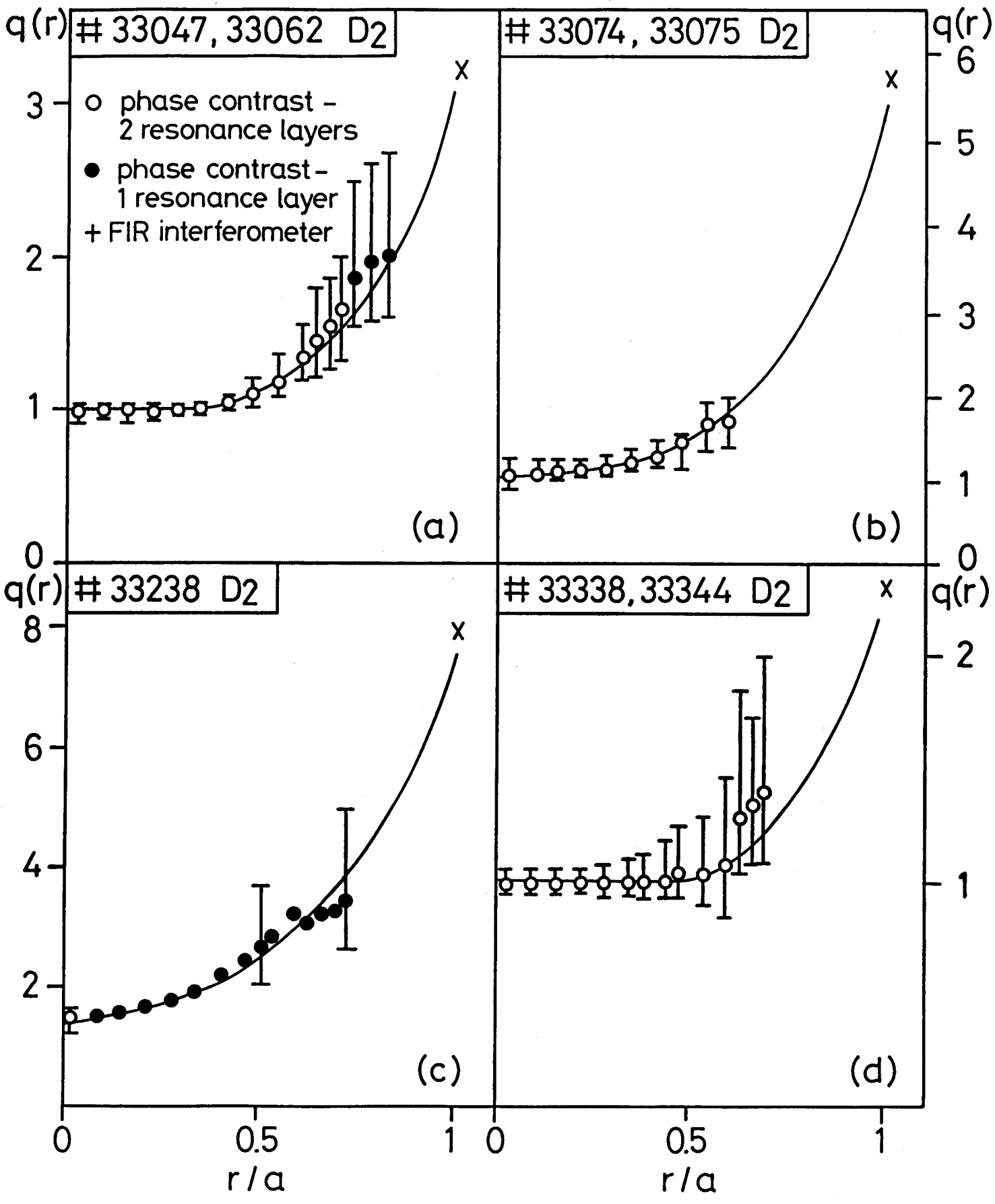
q(r)
# 33047, 33062 D2
o phase contrast – 2 resonance layers
● phase contrast – 1 resonance layer
+ FIR interferometer
x
(a)
33074, 33075 D2
(b)
33238 D2
(c)
33338, 33344 D2
(d)
r/a
0
0.5
1

FIG 6